JACS
JOURNAL OF THE AMERICAN CHEMICAL SOCIETY
Communication
pubs.acs.org/JACS

Enforced Layer-by-Layer Stacking of Energetic Salts towards High-Performance Insensitive Energetic Materials

Jiaheng Zhang,[†] Lauren A. Mitchell,[‡] Damon A. Parrish,[‡] and Jean'ne M. Shreeve*[,†]

[†]Department of Chemistry, University of Idaho, Moscow, Idaho 83844-2343, United States
[‡]Naval Research Laboratory, 4555 Overlook Avenue, Washington, D.C. 20375, United States

Supporting Information

ABSTRACT: Development of modern high-performance insensitive energetic materials is significant because of the increasing demands for both military and civilian applications. Here we propose a rapid and facile strategy called the "layer hydrogen bonding pairing approach" to organize energetic molecules via layer-by-layer stacking, which grants access to tunable energetic materials with targeted properties. Using this strategy, an unusual energetic salt, hydroxylammonium 4-amino-furazan-3-yl-tetrazol-1-olate, with good detonation performances and excellent sensitivities, was designed, synthesized, and fully characterized. In addition, the expected unique layer-by-layer structure with a high crystal packing coefficient was confirmed by single-crystal X-ray crystallography. Calculations indicate that the layer-stacking structure of this material can absorb the mechanical stimuli-induced kinetic energy by converting it to layer sliding, which results in low sensitivity.

Layer-by-layer assembly of molecules is ubiquitous in the natural world. More importantly, the highly ordered structures formed in this way usually show fascinating material characteristics, which has inspired chemists to conduct intensive research on such systems. In this context, leading progress has been made in the construction of luminescent chromophores and organic semiconductors by the assembly of building blocks.[1] Meanwhile, such parallel face-to-face arrangements were also discovered in the crystal structures of some high-performance insensitive energetic materials (HIEMs) and found to greatly affect their physicochemical and detonation properties.[2] These energetic materials, such as 2,4,6-triamino-1,3,5-trinitrobenzene (TATB), 3,3′-diamino-4,4′-azofurazan (DAAzF), and 1,1-diamino-2,2-dinitroethene (FOX-7), are confirmed to have some key structural features, such as planar conjugated molecules and layered crystal packing with reasonable interlayer spacing.[3] However, unsolved challenges still remain in layer construction and direction control to avoid a herringbone motif or other low-order packing pattern. With this in mind, described herein is a rapid and facile strategy called the "layer hydrogen bonding pairing approach" for controlling the assembly of energetic molecules and enforcing layer-by-layer stacking in the solid state.

In the field of solid-state engineering, efforts toward molecular control have focused on the utilization of weak interactions between functional groups.[4] Of these interactions, hydrogen bonding remains the most reliable; numerous examples of hydrogen-bonding-promoted assemblies have been reported.[5] Basically, hydrogen bonding involves a donor and an acceptor containing an acidic hydrogen atom and an electronegative atom (N, O, F, etc.), respectively. In our design concept, a nearly flat molecule or ion is required; therefore, aromatic rings with nitro, amino, or azo functional groups are structurally preferred, while imino and methylene linkages should be avoided in molecular design. Based on acidic hydrogen atoms and electronegative atoms, a target molecule/ion is divided into several H-bond donor and acceptor units, each donor and acceptor unit including one or more acidic hydrogen atom(s) and electronegative atom(s), respectively. In general, for stable, highly dense energetic materials, the constituent molecule/ion should possess at least four units to cover four or more directions which form dense infinite two-dimensional networks. The core of this strategy is that HIEMs can be designed by stacking of infinite 2D layers in which sequence targets are connected by pairing H-bond donor−acceptor units. Therefore, an energetic compound with suitable complementary donor−acceptor units is another prerequisite of the approach. Using this approach, all three representative energetic molecules are assembled as successive infinite 2D layers, and each layer is built up through pairing units (Figure 1). More importantly, the predicted layer combination modes are consistent with their real crystal structures (Figures S2−S4). As a matter of fact, both TATB and DAAzF have other

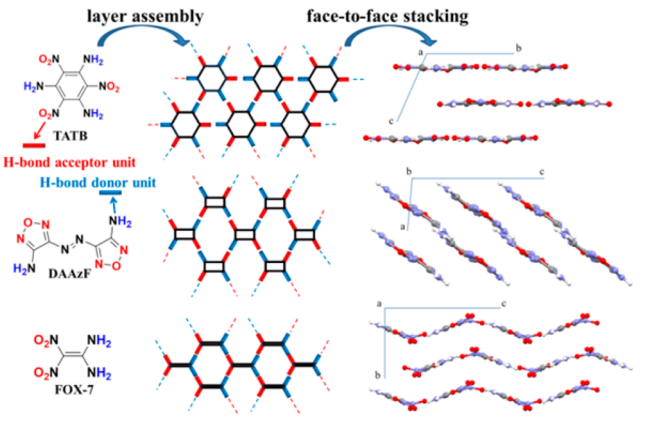

Figure 1. Schematic diagram of hydrogen-bonding-driven layer assembly and the face-to-face crystal packing for TATB, DAAzF, and FOX-7.

Received: July 27, 2015

DOI: 10.1021/jacs.5b07852
J. Am. Chem. Soc. XXXX, XXX, XXX−XXX

assembly modes; however, these modes are energetically less favorable and have less hydrogen bonding inside the pairing units (Figures S5 and S6). After the layer assembly, further interlinking of the 2D layers to 3D supramolecules is driven by π-stacked or other weak interactions in these cases.

After successful analysis of existing examples using the proposed approach, it was our intent to show that it can also be used to modify and design novel HIEMs. In this current work, 5-(4-amino-furazan-3-yl)-1-hydroxytetrazole (**1**) was chosen as a trial compound; based on its structure, this molecule contains three H-bond acceptor units and one donor unit. The composition of hydrogen bond donor−acceptor units in this target molecule represents a major class of energetic materials. In addition, the deprotonation of the N−OH moiety offers possibilities for structural modification. The synthesis process of **1** and detailed experimental steps are described in the Supporting Information. Judging by our strategy, this neutral compound is unable to evolve to a two-dimensional extension layer by itself because of the shortage of H-bond donor units for pairing. To verify this, a suitable crystal of **1** obtained by slow evaporation of a water solution was characterized by using single-crystal X-ray diffraction. Instead of obtaining a water-free structure, 5-(4-amino-furazan-3-yl)-1-hydroxytetrazole monohydrate was obtained. It is seen from the crystallographic data that compound **1** as well as one molecule of water forms in a monoclinic system $P21/n$ with four pairs of molecules per unit cell (Figure S7). However, even with pairing involving the extra two hydrogen bond donors from the water molecule, the packing diagram clearly shows zigzag stacking rather than a layer (Figures 2 and S8).

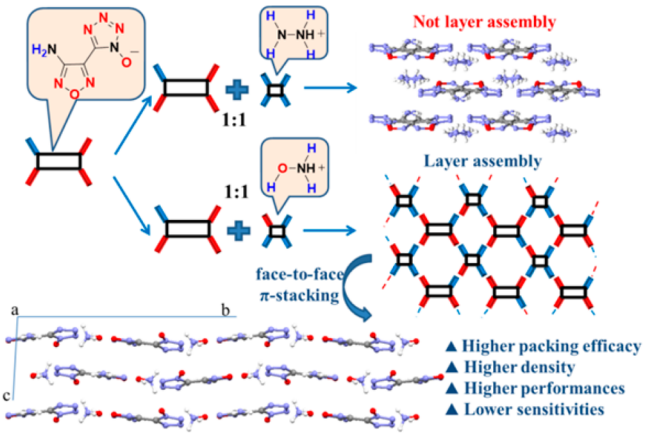

Figure 2. Layer assembly mode of hydroxylammonium 4-amino-furazan-3-yl-tetrazol-1-olate (**4**) and its crystal packing diagram.

As deduced from the proposed strategy, the balance of H-bond donor and acceptor units plays an important role in the layer assembly. However, most of the energetic compounds are structurally defined by nitrogen- and oxygen-containing heterocycles, N-oxide, and nitro groups, which are usually classified as H-bond acceptors.[6] Therefore, conformers to act as H-bond donor units are highly sought. We then carried out acid−base reactions and metathesis reactions using equimolar amounts of bases and hydrochloride salts of several guanidines, respectively, to prepare a series of energetic salts **2**−**10** (Scheme 1; see Supporting Information for detailed description). All the chosen cations are nitrogen-rich synthons that contain amino group(s) which are able to provide sufficient H-bond donor character.

Scheme 1. Synthesis of 5-(4-Amino-furazan-3-yl)-1-hydroxytetrazole-Based Energetic Salts

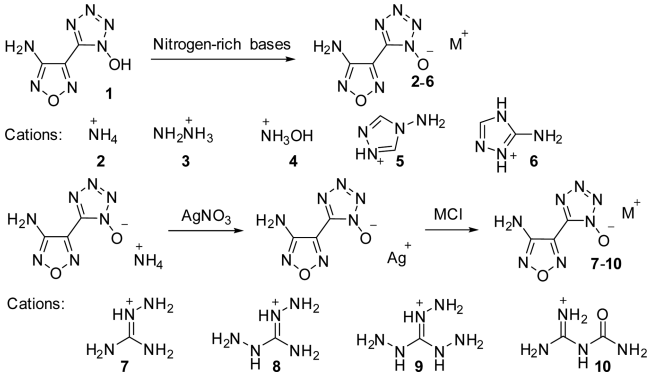

These ionic derivatives are isolated in nearly quantitative yields and are stable at room temperature for long periods. Characterization of these ionic energetic compounds was accomplished through IR spectroscopy, multinuclear NMR spectroscopy, and elemental analysis.

By applying the strategy to analysis of these newly prepared energetic salts, we believe that, instead of complete pairing, some cations provide excess bonding donor units, which might also result in an imbalance and a low-order packing pattern. For instance, hydrazinium salt (**3**) and diaminoguanidinium salt (**8**) have two or more NH_2 building blocks which can donate at least four acid hydrogens to form hydrogen bonds. The single-crystal X-ray structures of **3** and **8** confirm our assumption about their packing pattern (Figures S9 and S10). In order to pair these donor units, the 4-amino-furazan-3-yl-tetrazol-1-olate anion packs into a wavelike type for **3** and a crossing type for **8**. The dihedral angle between neighboring faces is 14.8° for **3** and 69.5° for **8** (Figure S11). After ruling out the possibility of these poly-amino cations, our requirements became clearer, i.e., a conformer with one H-bond acceptor unit and three donor units of its own.

Hydroxylammonium energetic salts belong to an important category of next-generation energetic materials. Among them, dihydroxylammonium 5,5′-bistetrazole-1,1′-diolate (TKX-50) and dihydroxylammonium 3,3′-dinitroamino-4,4′-azoxyfurazanate show impressive performances as promising candidates to replace currently used explosives; in addition, hydroxylammonium nitrate has already been used as a green propellant by the U.S. Army.[7] Different from other cations, the oxygen of the hydroxylammonium cation can not only increase the oxygen balance but also provide the acceptor character of the hydrogen bond. Meanwhile, the adjacent hydrogen and -NH_3 group of the hydroxylammonium cation can also act as three H-bond donor units for pairing with the 4-amino-furazan-3-yl-tetrazol-1-olate anion. In Figure 2 is displayed the perfect match of a predicted hydrogen-bonding-driven layer assembly by the hydroxylammonium cation and 4-amino-furazan-3-yl-tetrazol-1-olate anion. A suitable colorless crystal of **4** was obtained by slow recrystallization from an aqueous solution at room temperature, crystallizing in the monoclinic space group $P2_1/c$ with four molecules per unit cell. The geometry of the anion is comparable to that observed in its neutral precursor. The amino group and $N-O^-$ moiety lie in the plane of the furazan and tetrazole rings, as supported by the torsion angles (~180°). As expected, the arrangement of each layer is the same as the predicted mode in Figure 2. The dihedral angle between neighboring layers is exactly 0° for the crystal of **4**, which further confirms the parallel

DOI: 10.1021/jacs.5b07852
J. Am. Chem. Soc. XXXX, XXX, XXX−XXX

face-to-face arrangements (Figures S12 and S13). To identify the tightness of the assembly layers, the distances between furazan centroids and tetrazole centroids were measured to be 3.75 and 3.35 Å, respectively, both typical geometrical parameters of aromatic face-to-face π-interactions (<4.00 Å).[8] In addition to π-interactions, the assembly of the layers into a 3D supramolecular network also resulted from hydrogen bonding (1.72 Å) between the N−O$^-$ moiety from the upper anion and amino group from the bottom cation.

Both density and oxygen balance (oxygen content) play key roles in dictating the performances of explosives.[9] For common HIEMs, the oxygen balance is usually not very high because of the presence of amino group(s). Although they have a low ratio of heavy atoms (O, Cl, F, etc.), their densities usually reach very high values which are comparable to those of poly-nitro explosives. As a matter of fact, the increase in density is attributed not only to the substitution of heavy atoms/groups but also to an enhanced molecular packing efficiency in the solid state.[5a,10] This is clear from a comparison of packing coefficients (Table 1) for TATB, DAAzF, FOX-7, RDX, **1**, **3**, **4**, and **8**.

Table 1. Oxygen Content, Oxygen Balance (Ω), Calculated Packing Coefficients (PC), and Crystallographic Density for TATB, DAAzF, FOX-7, RDX, 1, 3, 4, and 8

material	oxygen content (%)	Ω[a] (%)	PC (%)	crystal density (g cm^{-3})
TATB	37.2	−55.8	78.1	1.938
DAAzF	16.3	−65.3	78.0	1.728
FOX-7	43.2	−21.6	78.0	1.907
RDX	43.2	−21.6	73.6	1.806
1[b]	25.7	−47.1	74.0	1.732
3	15.9	−59.7	74.0	1.706
4	23.8	−47.5	77.8	1.822
8[c]	12.4	−69.1	69.4	1.608

[a]Oxygen balance (based on carbon dioxide) for $C_aH_bO_cN_d$, $1600(c - a - b/2)/M_w$, where M_w = molecular weight. [b]The parameters of **1** were calculated with one lattice water. [c]The crystal data of **8** were collected at 296 K.

Because of the highly ordered layer-by-layer arrangements, the packing coefficients of TATB, DAAzF, FOX-7, and **4** are about 4% larger than the others and result in positive crystal density changes (~0.1 g cm^{-3}). The densities of **1**−**10** measured with a gas pycnometer at 25 °C (Table 2) are in agreement with the crystal data and follow a similar trend. Among them, **4** shows the uncommon distinction of being an energetic salt which has a slightly higher measured density than its nonionic precursor (**1**). It is worth mentioning that **10** possesses the second-highest measured density among the newly prepared energetic salts. Since the guanylurea cation also has one H-bond acceptor unit (carbonyl group) and three donor units (three amino groups), it is most likely that it can also assemble a layer structure similar to **4**, which leads to high packing efficiency and high density.

In this work, the heats of formation for **1** and the corresponding anion were obtained by using the isodesmic reaction approach. For energetic salts **2**−**10**, the solid-state heats of formation are calculated by employing Born−Haber energy cycles (see Supporting Information for calculation details).[11] Because of the presence of many N−N and N−O bonds, all compounds have highly endothermic enthalpies of formation in the range from 232.8 kJ mol^{-1} (**10**) to 760.9 kJ mol^{-1} (**5**). With measured density values and the calculated heats of formation in hand, detonation properties of **1**−**10** were obtained by

Table 2. Detonation Properties of Compounds 1−10 Compared with RDX and TATB

material[a]	D[b] (g cm^3)	$\Delta_f H$[c] (kJ g^{-1})	ν_D[d] (m s^{-1})	P[e] (GPa)	IS[f] (J)	FS[g] (N)
1	1.790	2.61	8601	30.0	37	>360
2	1.688	2.19	8436	26.6	>50	>360
3	1.695	2.79	8759	29.0	46	>360
4	1.803	2.25	9100	33.4	>50	>360
5	1.748	3.01	8600	28.0	>50	>360
6	1.736	2.47	8363	26.1	>50	>360
7	1.642	2.01	8173	23.6	>50	>360
8	1.689	2.30	8580	26.7	>50	>360
9	1.710	2.61	8859	29.0	45	>360
10	1.770	0.87	8303	25.3	>50	>360
RDX	1.820	0.36	8748	34.9	7.4	120
TATB	1.930	−0.54	8114	31.2	50	>360

[a]All the newly prepared materials are anhydrous for testing. [b]Density was measured by using a gas pycnometer at room temperature. [c]Calculated heat of formation. [d]Detonation velocity. [e]Detonation pressure. [f]Impact sensitivity. [g]Friction sensitivity.

employing EXPLO5 v6.01 (Table 2).[12] The detonation velocities and pressures lie in the ranges 8173−9100 m s^{-1} and 23.6−33.4 GPa, respectively. Compound **4** exhibits the highest detonation performances (ν_D = 9100 m s^{-1}; P = 33.4 GPa), which are significantly superior to those of TATB (ν_D = 8114 m s^{-1}; P = 31.2 GPa) and comparable to those of the highly explosive RDX (ν_D = 8748 m s^{-1}; P = 34.9 GPa). In addition, all salts exhibit excellent thermal stabilities (Supporting Information), which can be attributed to extensive hydrogen bonding interactions and strong cation−anion interactions. The decomposition temperatures for **2**−**10**, which fall in the range of 213−277 °C, are all higher than that of RDX (210 °C).

Impact and friction sensitivities (IS and FS, respectively) are high priorities for secondary explosives. Low sensitivities of energetic materials can reduce the risk of serious and fatal accidents during the manufacturing process and application.[13] In this work, the sensitivity values of **1**−**10** were determined by using standard Bundesanstalt für Materialforschung (BAM) techniques. All compounds show very low sensitivities toward mechanical stimulus (Table 2). Most of these salts have IS and FS greater than 50 J and 360 N, respectively. In the case of **4**, the good detonation performances coupled with relatively high thermal stability and excellent mechanical sensitivities suggest that this material may be an attractive HIEM candidate as a practical insensitive secondary explosive.

The sensitivities of energetic materials are related to the ease of self-sustaining hot spots which are caused by mechanical stimulus-induced lattice deformation (shear, slip, disorder, etc.).[14] It has been confirmed experimentally that explosives with certain geometries are able to minimize the deformation energy hot spots and act as desensitizers.[2a,15] To gain a better understanding of the desensitizing mechanism of layer-by-layer assembly HIEMs, a force field was established for **4** and RDX based on their unit cell geometries, and their abilities to handle external forces were probed (Figure 3; see Supporting Information for calculation details). For the purpose of convenient comparison, the value of external force is converted from mole units (kJ mol) into volume units (MJ m^3) by dividing by the simulated cell volume. According to our simulation, in the case of **4**, the internal stress along the a axis (0−76.0 MJ m^3) and the b axis (0−45.5 MJ m^3) is much lower than that along the c axis

DOI: 10.1021/jacs.5b07852
J. Am. Chem. Soc. XXXX, XXX, XXX−XXX

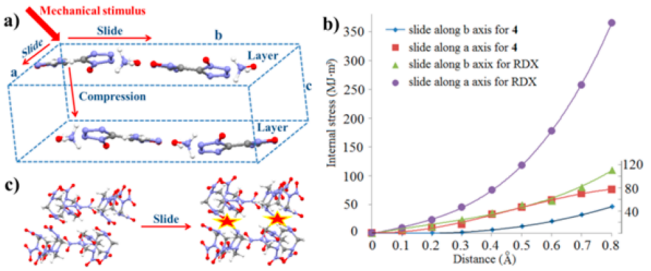

Figure 3. (a) Model for external forces acting on hydroxylammonium 4-amino-furazan-3-yl-tetrazol-1-olate (**4**) crystal unit cell. Any mechanical stimulus can be analyzed into three forces along three axes. (b) Internal stress curve along the *a* and *b* axes for **4** and RDX. (c) Plot showing the sliding constraint of the RDX crystal unit cell along the *b* axis.

(0−219.8 MJ m^3). It may be concluded that, in contrast to compression deformation, the layer-by-layer HIEMs can readily absorb mechanical stimuli by converting kinetic energy into layer sliding to prevent the formation of hot spots. This also should be the rationale for why high-performance insensitive energetic materials can be used as desensitizers versus mechanical stimuli. For comparison, the internal stress along the *a* axis and along the *b* axis for RDX is calculated to be 0−365.0 and 0−115.0 MJ m^3, respectively, indicating that the slide is highly restricted because of its packing mode.

In summary, we have developed a rapid and facile approach to design high-performance insensitive energetic materials, which is based on the hydrogen-bonding-promoted layer assembly of energetic molecules and therefore enforces layer-by-layer stacking in the solid state. By applying this strategy, a novel energetic material, hydroxylammonium 4-amino-furazan-3-yl-tetrazol-1-olate (**4**) was designed, synthesized, and fully characterized, which shows good detonation performances (ν_D = 9100 m s^{-1}; *P* = 33.4 GPa) and excellent sensitivities (IS > 50 J; FS > 360 N). The single-crystal X-ray structure of **4** confirmed expected layer-by-layer stacking, and the layer combination is exactly the same as in the design mode. These positive results suggest that this qualitative approach will enhance the future prospects for not only HIEMs design but also other solid-state materials. Computational analysis of internal stress indicates that the layer-by-layer geometries of HIEMs can readily absorb mechanical stimuli by convert kinetic energy into layer sliding and result in lower sensitivities.

■ ASSOCIATED CONTENT

Supporting Information

The Supporting Information is available free of charge on the ACS Publications website at DOI: 10.1021/jacs.5b07852.

Synthesis, characterization data, calculation details, and crystal refinements (PDF)
X-ray crystallographic files in CIF format for **1** (CIF)
X-ray crystallographic files in CIF format for **3** (CIF)
X-ray crystallographic files in CIF format for **4** (CIF)
X-ray crystallographic files in CIF format for **8** (CIF)

■ AUTHOR INFORMATION

Corresponding Author

*jshreeve@uidaho.edu

Notes

The authors declare no competing financial interest.

■ ACKNOWLEDGMENTS

Financial support from the Office of Naval Research (NOOO14-12-1-0536), the Defense Threat Reduction Agency (HDTRA 1-11-1-0034), and CFD Research Corporation is gratefully acknowledged.

■ REFERENCES

(1) Das, A.; Ghosh, S. *Angew. Chem., Int. Ed.* **2014**, *53*, 2038−2054.
(2) (a) Zhang, C.; Wang, X.; Huang, H. *J. Am. Chem. Soc.* **2008**, *130*, 8359−8365. (b) Zhang, C.; Xue, X.; Cao, Y.; Zhou, Y.; Li, H.; Zhou, J.; Gao, T. *CrystEngComm* **2013**, *15*, 6837−6844. (c) Zhang, J.; Zhang, Q.; Vo, T. T.; Parrish, D. A.; Shreeve, J. M. *J. Am. Chem. Soc.* **2015**, *137*, 1697−1704.
(3) Ma, Y.; Zhang, A.; Zhang, C.; Jiang, D.; Zhu, Y.; Zhang, C. *Cryst. Growth Des.* **2014**, *14*, 4703−4713.
(4) (a) Wood, P. A.; Feeder, N.; Furlow, M.; Galek, P. T. A.; Groom, C. R.; Pidcock, E. *CrystEngComm* **2014**, *16*, 5839−5848. (b) Zhang, J.; Parrish, D. A.; Shreeve, J. M. *Chem. Commun.* **2015**, *51*, 7337−7340.
(5) (a) Landenberger, K. B.; Bolton, O.; Matzger, A. J. *J. Am. Chem. Soc.* **2015**, *137*, 5074−5079. (b) Landenberger, K. B.; Bolton, O.; Matzger, A. J. *Angew. Chem., Int. Ed.* **2013**, *52*, 6468−6471. (c) Bolton, O.; Matzger, A. J. *Angew. Chem., Int. Ed.* **2011**, *50*, 8960−8963.
(6) (a) Klapötke, T. M.; Schmid, P. C.; Schnell, S.; Stierstorfer, J. *Chem. - Eur. J.* **2015**, *21*, 9219−9228. (b) Dippold, A. A.; Klapötke, T. M. *J. Am. Chem. Soc.* **2013**, *135*, 9931−9938. (c) Zhang, Q.; Zhang, J.; Qi, X.; Shreeve, J. M. *J. Phys. Chem. A* **2014**, *118*, 10857−10865.
(7) (a) Zhang, J.; Shreeve, J. M. *J. Am. Chem. Soc.* **2014**, *136*, 4437−4445. (b) Fischer, N.; Fischer, D.; Klapötke, T. M.; Piercey, D. G.; Stierstorfer, J. *J. Mater. Chem.* **2012**, *22*, 20418−20422. (c) Witze, A. *Nature* **2013**, *500*, 509−510.
(8) Molčanov, K.; Sabljić, I.; Kojić-Prodić, B. *CrystEngComm* **2011**, *13*, 4211−4217.
(9) (a) Fischer, D.; Klapötke, T. M.; Stierstorfer, J. *Angew. Chem., Int. Ed.* **2015**, DOI: 10.1002/anie.201502919. (b) Wu, Q.; Zhu, W.; Xiao, H. *J. Mater. Chem. A* **2014**, *2*, 13006−13015. (c) Zhang, J.; Shreeve, J. M. *J. Phys. Chem. C* **2015**, *119*, 12887−12895. (d) Shen, C.; Wang, P.; Lu, M. *J. Phys. Chem. A* **2015**, *119*, 8250−8255.
(10) Aakeröy, C. B.; Wijethunga, T. K.; Desper, J. *Chem. - Eur. J.* **2015**, *31*, 11029−11037.
(11) Jenkins, H. D. B.; Tudela, D.; Glasser, L. *Inorg. Chem.* **2002**, *41*, 2364−2367.
(12) Sućeska, M. *EXPLO5*, v6.01; Brodarski Institute: Zagreb, Croatia, 2013.
(13) (a) Politzer, P.; Murray, J. S. *Adv. Quantum Chem.* **2014**, *69*, 1−30. (b) Politzer, P.; Murray, J. S. *Cryst. Growth Des.* **2015**, *15*, 3767−3774. (c) Badgujar, D. M.; Talawar, M. B.; Asthana, S. N.; Mahulikar, P. P. *J. Hazard. Mater.* **2008**, *151*, 289−305.
(14) Politzer, P.; Murray, J. S. *J. Mol. Model.* **2015**, *21*, 25−36.
(15) (a) An, Q.; Liu, Y.; Zybin, S. V.; Kim, H.; Goddard, W. A. *J. Phys. Chem. C* **2012**, *116*, 10198−10206. (b) Sharia, O.; Tsyshevsky, R.; Kuklja, M. M. *J. Phys. Chem. Lett.* **2013**, *4*, 730−734. (c) Aluker, E. D.; Krechetov, A. G.; Mitrofanov, A. Y.; Zverev, A. S.; Kuklja, M. M. *J. Phys. Chem. C* **2012**, *116*, 24482−24486.

DOI: 10.1021/jacs.5b07852
J. Am. Chem. Soc. XXXX, XXX, XXX−XXX